Original Article
The inhibitory and transcriptional effects of the epigenetic repurposed drugs hydralazine and valproate in lymphoma cells

Harold Salamanca-Ortiz[1*], Guadalupe Domínguez-Gomez[3*], Alma Chávez-Blanco[1], Daniel Ortega-Bernal[4,5,6], José Díaz-Chávez[1], Aurora González-Fierro[1], Myrna Candelaria-Hernández[3], Alfonso Dueñas-González[1,2]

[1]Subdirection of Basic Research, Instituto Nacional de Cancerología (INCan), Tlalpan, Mexico City 14080, Mexico; [2]Department of Genomic Medicine and Environmental Toxicology, Institute of Biomedical Research, Universidad Nacional Autónoma de Mexico (UNAM), Av. Universidad 3004, Copilco Universidad, Coyoacan, Mexico City 04510, Mexico; [3]Subdirección de Investigación Clínica, Instituto Nacional de Cancerología (INCan), Tlalpan, Mexico City 14080, Mexico; [4]Departamento de Ciencias Naturales, Unidad Cuajimalpa, Universidad Autónoma Metropolitana, Coyoacan, Mexico City 05348, Mexico; [5]Department of Sciences, Universidad Autónoma Metropolitana, Coyoacan, Mexico City 04960, Mexico; [6]Departamento de Atención a la Salud, Universidad Autónoma Metropolitana Xochimilco, Coyoacan, Mexico City 04960, Mexico. *Equal contributors.

Abstract: Lymphoma is a disease that affects countless lives each year. In order to combat this disease, researchers have been exploring the potential of DNMTi and HDACi drugs. These drugs target the cellular processes that contribute to lymphomagenesis and treatment resistance. Our research evaluated the effectiveness of a combination of two such drugs, hydralazine (DNMTi) and valproate (HDACi), in B-cell and T-cell lymphoma cell lines. Here we show that the combination of hydralazine and valproate decreased the viability of cells over time, leading to the arrest of cell-cycle and apoptosis in both B and T-cells. This combination of drugs proved to be synergistic, with each drug showing significant growth inhibition individually. Microarray analyses of HuT 78 and Raji cells showed that the combination of hydralazine and valproate resulted in the up-regulation of 562 and 850 genes, respectively, while down-regulating 152 and 650 genes. Several proapoptotic and cell cycle-related genes were found to be up-regulated. Notably, three and five of the ten most up-regulated genes in HuT 78 and Raji cells, respectively, were related to immune function. In summary, our study suggests that the combination of hydralazine and valproate is an effective treatment option for both B- and T-lymphomas. These findings are highly encouraging, and we urge further clinical evaluation to validate our research and potentially improve lymphoma treatment.

Keywords: Non-Hodgkin lymphoma, hydralazine, valproate

Introduction

Non-Hodgkin lymphoma (NHL) is a diverse group of lymphocyte-derived malignancies with heterogeneous molecular features and clinical manifestations. DNA hypermethylation and histone deacetylation in B-cell and T-cell lymphomas are common, and these alterations contribute to lymphomagenesis [1, 2]. Despite the strong rationale for using a combination of DNA methyltransferase (DNMTi) and histone deacetylase (HDACi) inhibitors in NHL, no DNMTi has been FDA-approved, whereas among HDACi vorinostat and romidepsin are approved for cutaneous T-cell lymphoma (CTCL), and panobi-

nostat for peripheral T-cell lymphoma respectively [3].

The antihypertensive drug hydralazine (H) has been repositioned as a DNMTi, while valproate (V) is an antiepileptic drug repositioned as an HDACi. Phase I clinical trials of these agents, alone or in combination, have shown they are well tolerated [4-6]. These agents have clinically shown efficacy in myelodysplastic syndrome [7, 8] and cutaneous T-cell lymphoma [9]. On one hand, in NHL, the nucleoside analogs azacitidine and decitabine have limited clinical efficacy as single agents [10-12]. However, a DNMTi, combined with standard R-CHOP,

increases the response rate and is well-tolerated [13, 14]. Likewise, the HDACi vorinostat has modest efficacy as a single agent in relapsed NHL [15, 16]. Additionally, HDACi shows synergistic activity when combined with anti-CD20 monoclonal antibodies, proteasome inhibitors, or immunomodulatory agents [17, 18]. HDACi's mixed efficacy and toxicity results are observed when these agents are combined with cytotoxic chemotherapy [19-21]. However, a more recent study, combining valproate with R-CHOP as first-line therapy in diffuse large B-cell lymphoma [DLBCL], resulted in higher efficacy than historical controls [22]. These findings hold promise for the potential of the hydralazine valproate combination in reducing cell viability, inducing cell cycle arrest and apoptosis, and showing the synergistic effect of the combination in inhibiting lymphoma cell growth.

DNMTi and HDACi synergize regarding antitumor effects and gene expression [23, 24]. Hence, this has led to preclinical and clinical studies combining DNMTi, decitabine, or azacytidine with vorinostat or other HDACIs. In MDS and AML, results are encouraging [25], and in NHL, Pera et al. reported that the vorinostat and azacitidine combination appears to have a delayed chemosensitization effect [26].

While the HV combination has shown preclinical and clinical efficacy in T-cell NHL [9, 27], its activity has not yet been evaluated in B-cell lymphoma. This study presents a novel evaluation of the anti-lymphoma efficacy of the combination of hydralazine valproate (HV) in B lymphoma cell lines in vitro.

Materials and methods

Cell lines, culture, and drugs

We used the following cell lines: Non-Hodgkin's B cell lymphoma Raji, Nawalma, SU-DHL-10, and CA46, as well as the cutaneous T-cell lymphoma HuT 78. Cells were obtained from the American Type Culture Collection (Manassas, VA, USA). Cells were cultured at 37°C in a humidified atmosphere containing 5% CO_2 with RPMI-1640 medium supplemented with 10% fetal bovine serum (both Gibco BRL, Gaithersburg, MD) and 1% antibiotic-antimycotic solution (10,000 U/ml penicillin, 10.000 μg/ml streptomycin and 25 μg/ml de amphotericin B, Corning). Hydralazine was purchased from

Sigma-Aldrich (Merck KGaA, Darmstadt, Germany), and magnesium valproate was purchased from Psicofarma S.A. de CV, Mexico.

Cell viability after treatment with the hydralazine valproate combination

In our study, we seeded a total of 7×10^5 Raji cells and 1×10^5 HuT 78, Nawalma, SU-DHL-10, or CA46 cells into 24-well plates. These cells were then treated with either hydralazine or valproate at escalating doses, with the fresh, complete medium containing each drug changed every 24 hours. After 72 hours of treatment, we recovered and resuspended the pellets in 1 mL RPMI-1640 medium to assess cell viability using a trypan blue exclusion assay in a TC10TMAutomated Cell Counter (BioRad). Viable cells (%) = total number of viable cells per ml of aliquot/total number of cells per ml of aliquot × 100. The cytotoxic effect of each treatment was expressed as a percentage of cell viability relative to untreated control cells and is defined as treated cells/non-treated cells × 100.

The Inhibitory Concentration (IC) IC_{10} through IC_{50} values were obtained from the dose-response curves at different concentrations per drug using the four-parameter logistic function classical in the SigmaPlot software 10.0.

The combined treatments were carried out with hydralazine and valproate. Cells were seeded in a complete medium and, after 24 hours of incubation, treated with hydralazine 10 μM and valproate 1 mM for 168 hours with daily changes of drug-containing media. After 168 hours of treatment, cell viability was determined by trypan blue exclusion assay, as described above. This rigorous methodology ensures the reliability and validity of our findings.

Flow cytometry analysis of cell cycle and apoptosis after treatment with the hydralazine valproate combination

Cells were seeded in 25-cm² culture flasks (Corning Inc., Corning, NY, USA) at 2×10^5 cells/mL density and treated with hydralazine 10 μM and valproate 1 mM. After 72 h for HuT 78 and 48 h for Raji, cells were stained with propidium iodide (Sigma) and analyzed for DNA content on the flow cytometer BD FACSCanto™ II (BD Biosciences). Debris and aggregates were

gated out during data acquisition, and 20,000 gated events were collected for each sample. Cell cycle analyses were performed employing the ModFit LT software (Verity Software House). For apoptosis, 1×10^6 cells were resuspended in binding buffer, and 100 µL of this solution was transferred into a 5 mL tube, adding 5 µL of FITC Annexin V and 5 µL of propidium iodide. According to the manufacturer's instructions, apoptotic cells were detected by flow cytometry using the Annexin V-FITC Apoptosis Detection Kit (Sigma). Flow cytometric experiments were carried out using the BD FACSCanto™ II (BD Biosciences) flow cytometer.

Pharmacological interaction

Increasing doses of hydralazine (IC_{10}, IC_{20}, IC_{30}, IC_{40}, and IC_{50}) were combined with their respective increasing doses of valproate (IC_{10}, IC_{20}, IC_{30}, IC_{40}, and IC_{50}). The resulting mixtures (HV IC_{10}, HV IC_{20}, HV IC_{30}, HV IC_{40}, HV IC_{50}) were employed for viability curve assays. Cells were seeded into 24-well plates: 7×10^5 Raji cells, 1×10^5 HuT 78, Nawalama, SU-DHL-10, or CA46 cells in 1 mL of complete medium and then treated for 72 hours with the different combinations of the ICs of HV, pellets were recovered and resuspended in 1 mL of culture medium to assess cell viability by trypan blue exclusion assay. HV interactions were determined using the combination index (CI) method from Chou and Talalay's mathematical formula (CalcuSyn software, Biosoft). The CI is a numerical representation of pharmacological interaction, which considers each drug's dose-response curve and the drug combinations' growth inhibition curve to determine synergism, addition, or inhibition. This model uses the formula: fa/fu = [D/Dm], where fa is the fraction of cells inhibited, fu = 1-fa, the unaffected fraction, D is the concentration of the drug, Dm is the potency of the drug, and m is the shape of the dose-effect curve.

Statistical analyses

Three independent experiments were carried out in triplicate, and data was expressed as the mean ± standard deviation. Data were statistically analyzed using GraphPad Prism V6 software (GraphPad Software Inc., La Jolla, CA, USA). Significant differences were determined using one-way analysis of variance (ANOVA) followed by Dunnett correction to determine significant differences between each experimental group against its respective control. $P < 0.05$ was considered to be a statistically significant difference.

Microarrays and gene expression analysis

HuT 78 and Raji cells were treated as above, and then total RNA was isolated using TRIzol (Thermo Fisher Scientific, Inc.), according to the manufacturer's protocols. RNA quality was evaluated by capillary electrophoresis (Agilent 2100 Bioanalyzer, Agilent Technologies, Inc., Santa Clara, CA, USA); only RNA samples with an RNA integrity number >8.0 were further processed for microarray analysis. 200 ng RNA from each experimental cell group was evaluated using the Gene Chip Human Transcriptome Array 2.0 (Affymetrix; Thermo Fisher Scientific, Inc.) to determine the whole transcriptome expression profiles manufacturer's protocols. Briefly, the synthesis and amplification of cDNA and gene expression profiling were conducted using the WT PLUS Reagent Kit for fresh samples (Affymetrix; Thermo Fisher Scientific, Inc.). The samples were washed and stained using the Gene Chip hybridization wash and stain kit in the Gene Chip Fluidics Station 450 system (Affymetrix; Thermo Fisher Scientific, Inc.). The probe arrays were scanned using The Gene Chip Scanner 30007G (Affymetrix; Thermo Fisher Scientific, Inc.). Signal intensities of the array were analyzed with Affymetrix Expression Console software (version 1.3). Briefly, raw data probes were normalized using Signal Space Transformation-Robust Multichip Analysis for background correction and to obtain the quantile algorithm. To define the different conditions' differential expression profiles, two-way ANOVA was performed in the Affymetrix Transcriptome Analysis Console software (version 4.0). Genes with a fold change >1.4 or <-1.4 and an FDR<0.05 were considered significantly altered between the conditions. All data were uploaded in Gene Expression Omnibus: GSE168790.

Gene set enrichment analysis (GSEA)

GSEA was used to determine whether a priori-defined set of genes derived from annotation or pathway databases exhibited statistically significant differential expression. The analysis used the Ingenuity® Pathway Analysis tool (IPA®, Qiagen, Inc., Valencia, CA, USA). We used the

following thresholds for pathways selection: -log(P-value) >1.3 (P-value <0.05) and a |z-score| >1.

RT-qPCR

HuT 78 and Raji cells were treated as above, and total RNA was isolated when cells attained ~70% confluence, using TRIzol reagent according to the manufacturer's protocols. RNA purity and integrity were assessed via spectrophotometric analysis using a NanoDrop 2000c spectrophotometer (NanoDrop Technologies; Thermo Fisher Scientific, Inc.) using a MiniBIS Pro D-Transilluminator (DNR Bio-Imaging Systems Ltd., Neve Yamin, Israel). A total of 1 µg RNA was used for cDNA synthesis with the GeneAmp RNA PCR Core kit (Applied Biosystems; Thermo Fisher Scientific, Inc.). iQ SYBR Green SuperMix (Bio-Rad Laboratories, Inc.) was used according to the manufacturer's protocols. qPCR reactions were triplicated using an ABI Prism 7000 (Applied Biosystems; Thermo Fisher Scientific, Inc.). The thermocycling conditions for qPCR were as follows: 10 min at 95°C, 40 cycles of 30 sec at 95°C, and 30 sec at 60°C. Data were analyzed using the 2-ΔΔCq method [12] and reported as the fold-change in gene expression normalized to the endogenous control gene hypoxanthine phosphoribosyltransferase 1 (*HPRT1*) and relative to untreated cells. The primers used were: *HPRT1* forward, 5'-GAA CCT CTC GGC TTT CCC G-3' and reverse, 3'-CAC TAA TCA CGA CGC CAG GG-5'; *STAT-1* forward, 5'-ATG CTG GCA CCA GAA CGA AT-3' and reverse, 3'-GCT GGC TGA CGT TGG AGA TC-5'; and *SCD* forward, 5'-GGG ATC CTT CAG CAC AGG AA-3' and reverse, 3'-CAC CGC TTC TCC AAT GGA TT-5'; *FASN* forward, 5'-GTT CTG GGA CAA CCT CAT C-3' and reverse, 5'-CGA AGA AGG AGG CAT CAA-3. Annealing temperatures were 60°C for all reactions. Three independent triplicates were conducted. *P*-values were calculated using a two-tailed t-test.

Results

Cell viability analysis of the combination

The results from the HV combination treatment on cell viability are shown in **Figure 1**. In HuT 78 cells, maximal inhibition of 68% was observed at 168 hours, whereas in all B-cell lymphoma cell lines, almost complete inhibition occurred between 72 and 120 hours.

Cell cytometry analysis

Cells were analyzed by flow cytometry to evaluate the effect of hydralazine and valproate on the cell cycle and apoptosis. HuT 78 cells were mainly arrested in G2/M, whereas in Raji cells, the most significant effect was an arrest in the G1 phase. There was a statistically significant increase in apoptosis in both cell lines compared to controls, around 20% in both HuT 78 and Raji cells (**Figure 2**).

Cell viability analysis of individual drugs

To demonstrate that the epigenetic agents, hydralazine and valproate, individually decrease the cellular viability of the lymphoma cell lines, cells were treated with increasing doses of hydralazine and valproate. As shown in **Figure 3**, hydralazine promotes inhibition of cell viability at all doses in HuT 78, with maximal inhibition at 50 µM. Raji cells were significantly inhibited at all doses with maximal inhibition at 50 µM. In Nawalma cells, inhibition was observed only with 40 µM and 50 µM. Significant inhibition starting at 20 µM and a higher inhibition at 50 µM was observed in SU-DHL-10 and CA46 cell lines. Valproate inhibited cell viability at all tested doses in a dose-dependent manner. At a dose between 1 and 3 mM, the inhibition was nearly complete in all B-cell lymphoma cell lines. The T-cell lymphoma cells showed lower inhibition than B-cells. Nevertheless, inhibition was close to 70% at 2 mM and 3 mM.

Pharmacological interaction for synergy

The pharmacological interaction analyses showed that treatment of HuT 78 and Raji cells showed higher synergy, observed at all ICs tested (CI<1). In the CA46 cell line, synergy was observed with IC_{10} and IC_{20}, whereas at IC_{50}, the synergy was borderline (close to CI 1). Borderline synergy was observed with IC_{40} and IC_{50} in SU-DHL-10 cells. No synergy was observed in Nawalma. However, the lower bars at IC_{30}, IC_{40}, and IC_{50} suggest that the combination maintained its inhibitory effect (**Figure 4**).

Gene expression analysis

562 and 152 genes were up- and down-regulated, respectively, in HuT 78 cells. Treatment of Raji cells showed 850 up-regulated and 650 down-regulated genes. Volcano plots show the
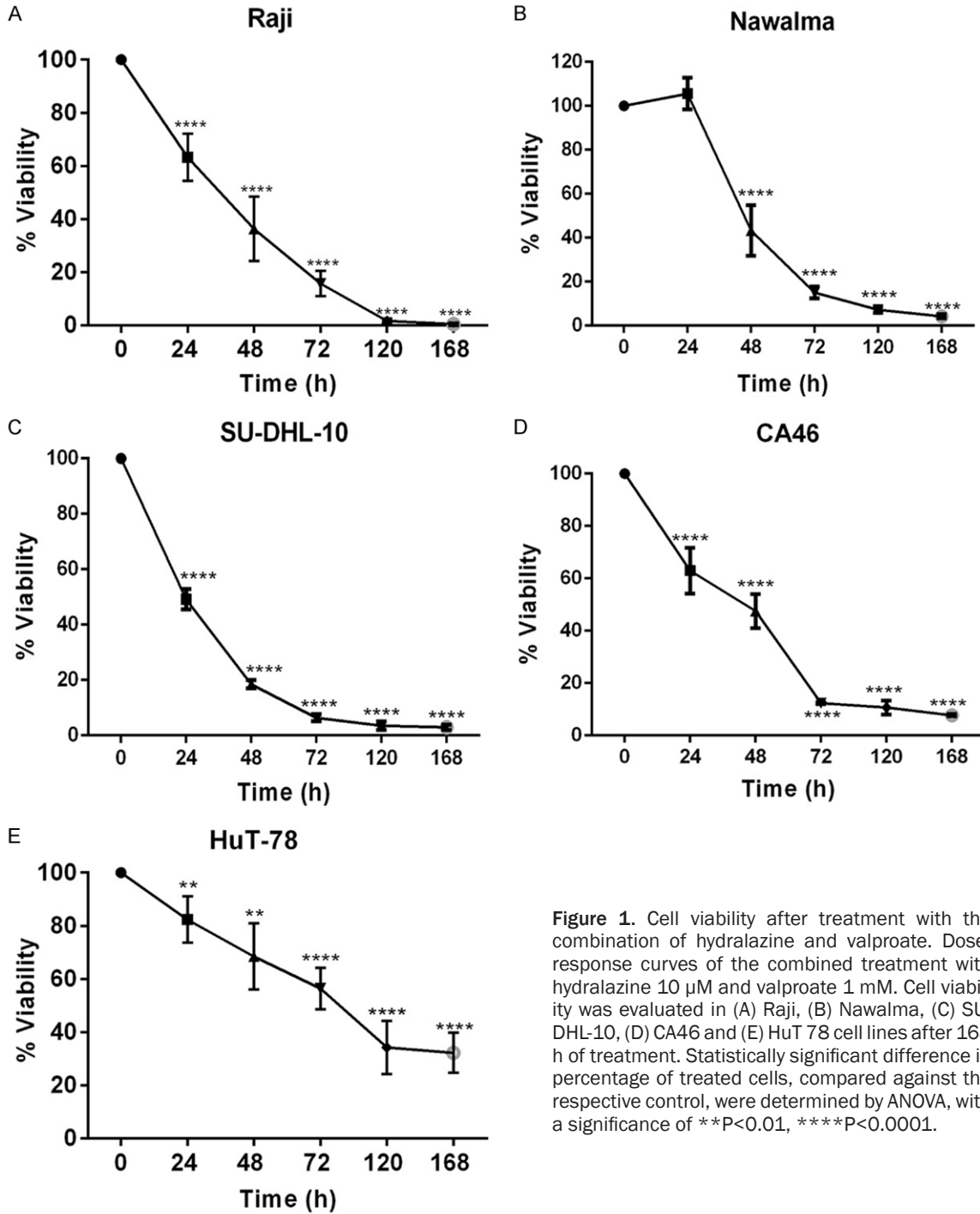
Figure 1. Cell viability after treatment with the combination of hydralazine and valproate. Dose-response curves of the combined treatment with hydralazine 10 µM and valproate 1 mM. Cell viability was evaluated in (A) Raji, (B) Nawalma, (C) SU-DHL-10, (D) CA46 and (E) HuT 78 cell lines after 168 h of treatment. Statistically significant difference in percentage of treated cells, compared against the respective control, were determined by ANOVA, with a significance of **P<0.01, ****P<0.0001.

differentially expressed genes with an FDR< 0.05 and a fold change >1.4 or <-1.4. The red and green points in the plot indicate >1.4-fold upregulation and downregulation of expression with statistical significance (**Figure 5**).

Table 1 lists the top ten up-regulated genes in HuT 78 and Raji cells. In HuT 78 cells, three

were genes related to antigen processing (TLR6), innate immunity, and gamma interferon signaling (*LAIR2 and GBP2*). Similarly, five out of the top ten up-regulated genes in Raji cells are related to immune function (chemokine, *CXCL10*; *IF16, IFN-gamma* and innate immunity; Immunoglobulin heavy chain, *IGHV1-24*; and Interferon-induced proteins *IFIT1, IFI4*). Several
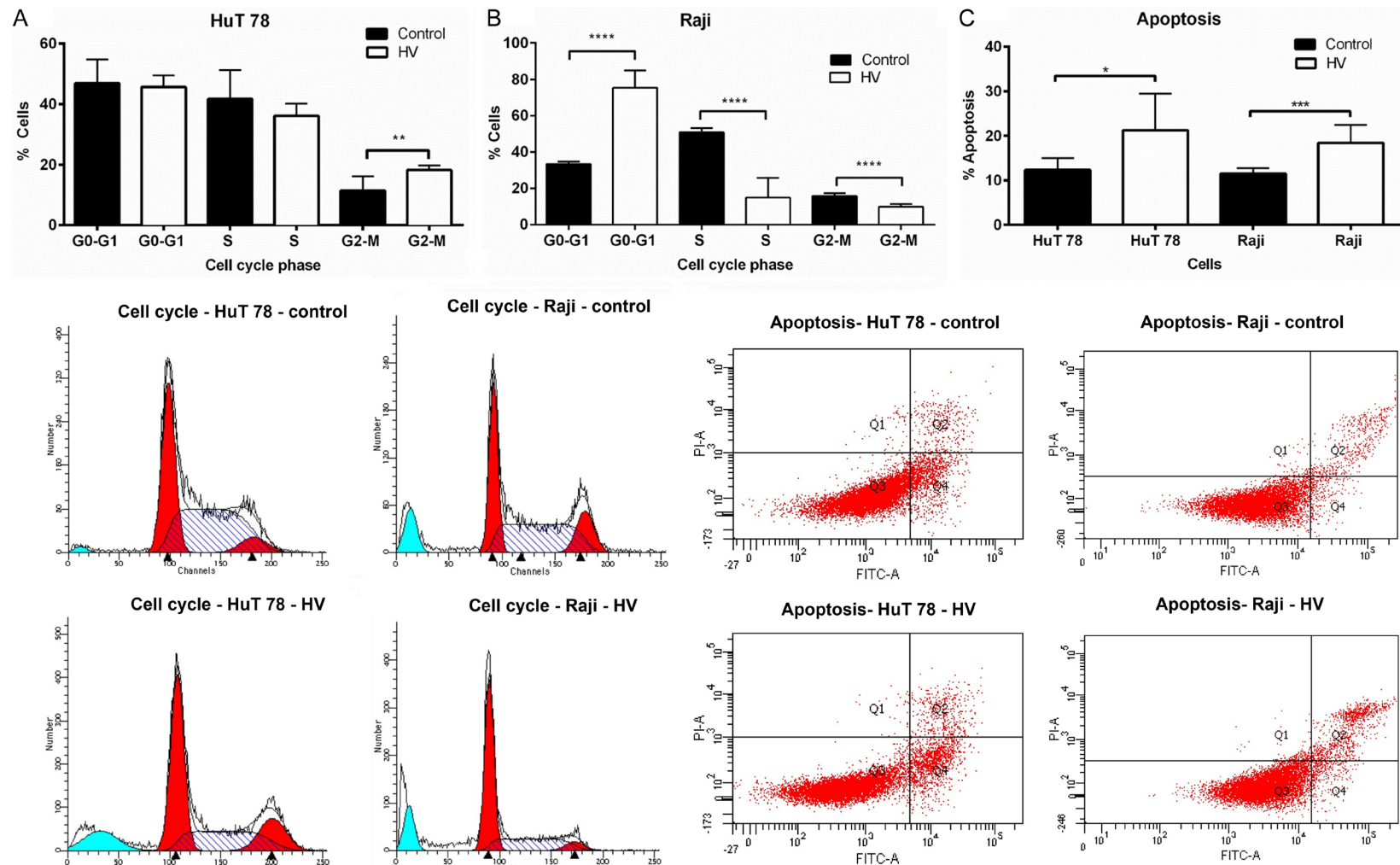
Figure 2. Cell cycle and apoptosis after treatment with combined hydralazine and valproate. The hydralazine and valproate combination induces cell cycle cell arrest and increased apoptosis. A. Cell cycle phase of HuT 78 cells was determined after treatment with hydralazine (10 µM) and valproate (1 mM) for 72 h and 48 h, respectively. Statistically significant differences in the percentage of cells in each phase of cell cycle (**, P = 0.0024) were determined by unpaired t test with a significance level of P<0.05. B. Cell cycle phase of Raji cells was determined after treatment with hydralazine (10 µM) and valproate (1 mM) for 72 h and 48 h, respectively. Statistically significant differences in the percentage of cells in each phase of cell cycle (****, P = 0.0001) were determined by unpaired t test with a significance level of P<0.05. C. Apoptotic cells were analyzed using Annexin-V and propidium iodide. Statistically significant percentages of apoptotic cells in HuT 78 (*, P = 0.0264) and Raji (***, P = 0.0004) cell lines were determined by an unpaired t test with a significance level of (P<0.05).
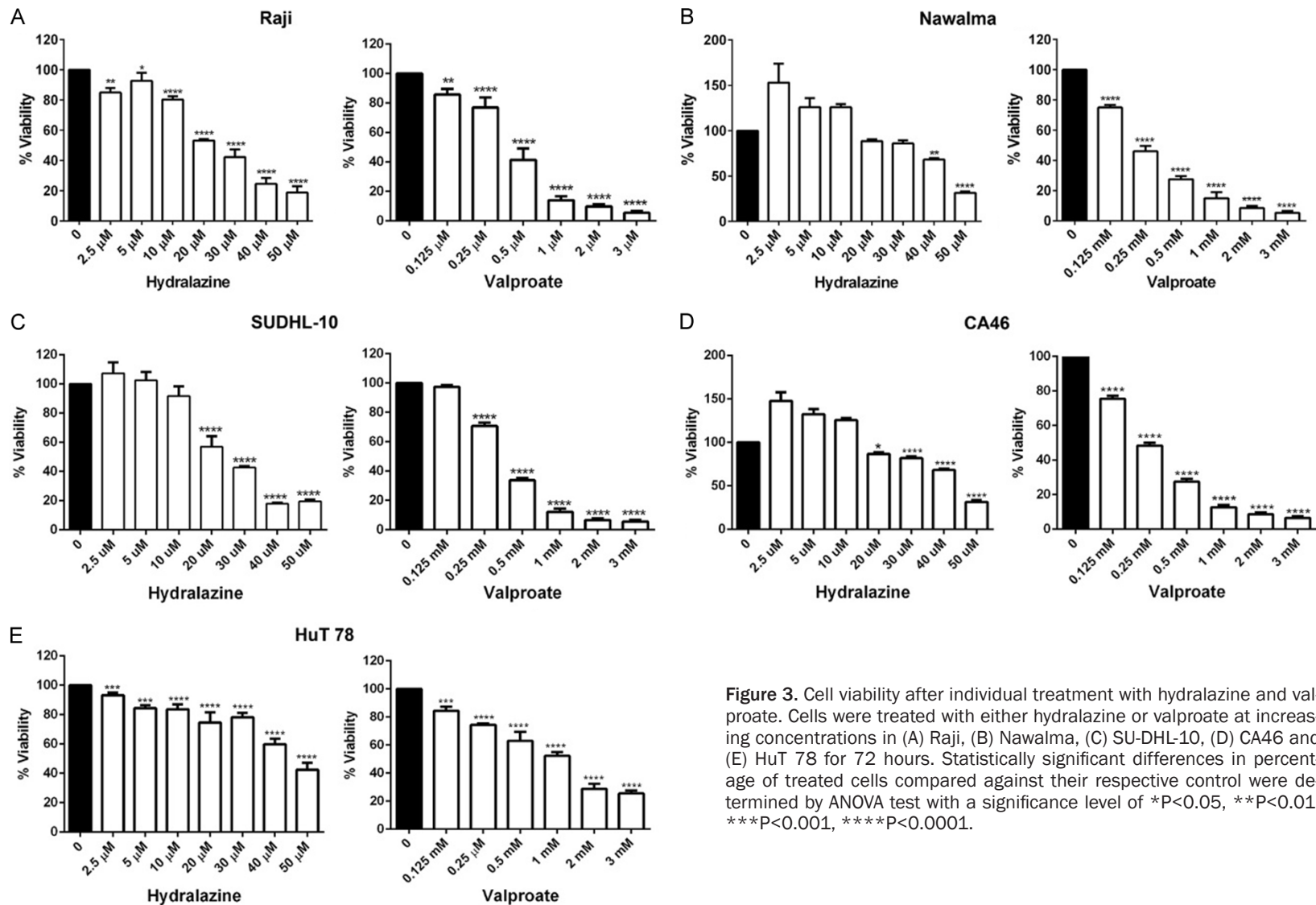
Figure 3. Cell viability after individual treatment with hydralazine and valproate. Cells were treated with either hydralazine or valproate at increasing concentrations in (A) Raji, (B) Nawalma, (C) SU-DHL-10, (D) CA46 and (E) HuT 78 for 72 hours. Statistically significant differences in percentage of treated cells compared against their respective control were determined by ANOVA test with a significance level of *P<0.05, **P<0.01, ***P<0.001, ****P<0.0001.
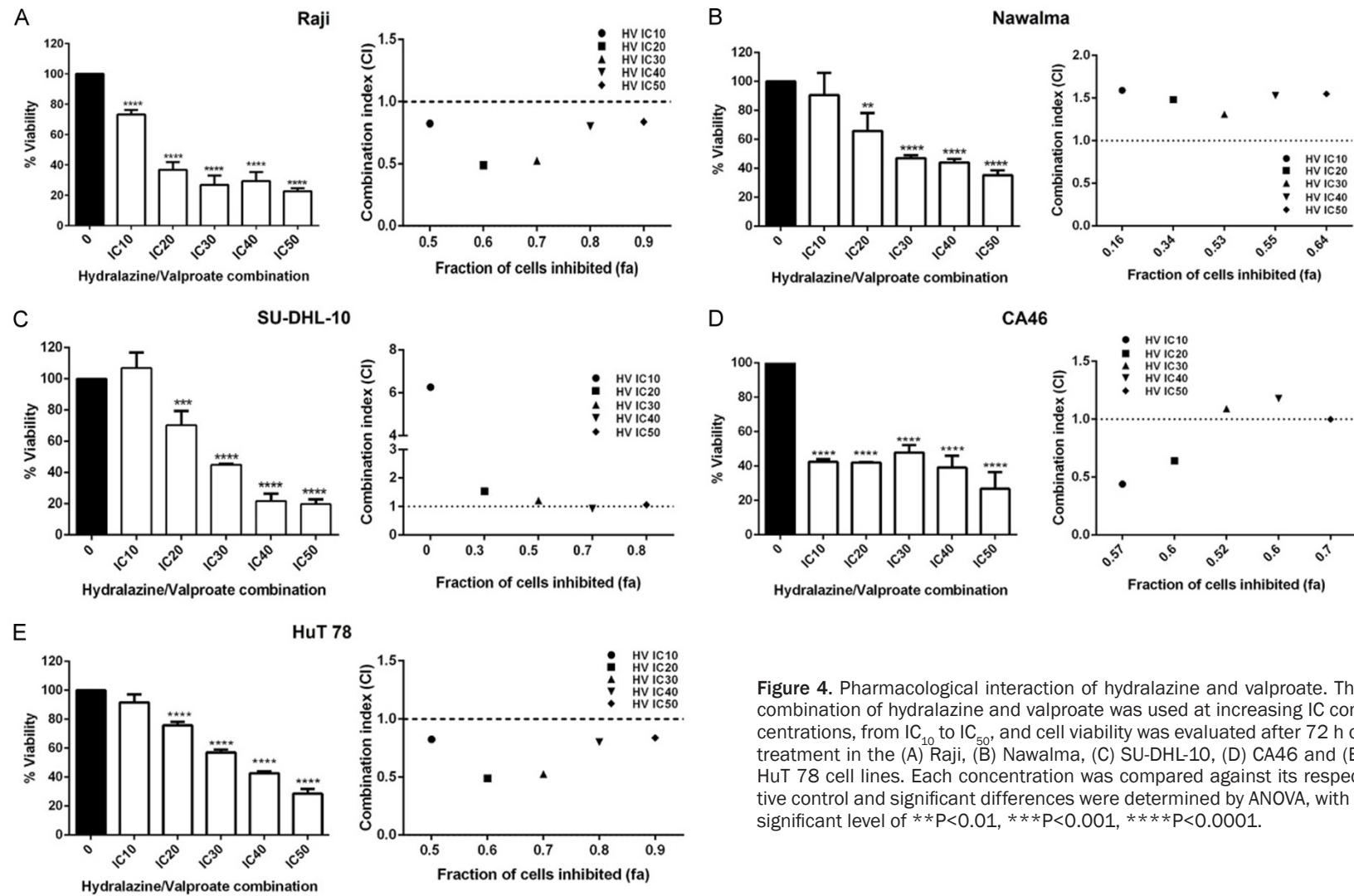
Figure 4. Pharmacological interaction of hydralazine and valproate. The combination of hydralazine and valproate was used at increasing IC concentrations, from IC_{10} to IC_{50}, and cell viability was evaluated after 72 h of treatment in the (A) Raji, (B) Nawalma, (C) SU-DHL-10, (D) CA46 and (E) HuT 78 cell lines. Each concentration was compared against its respective control and significant differences were determined by ANOVA, with a significant level of **P<0.01, ***P<0.001, ****P<0.0001.
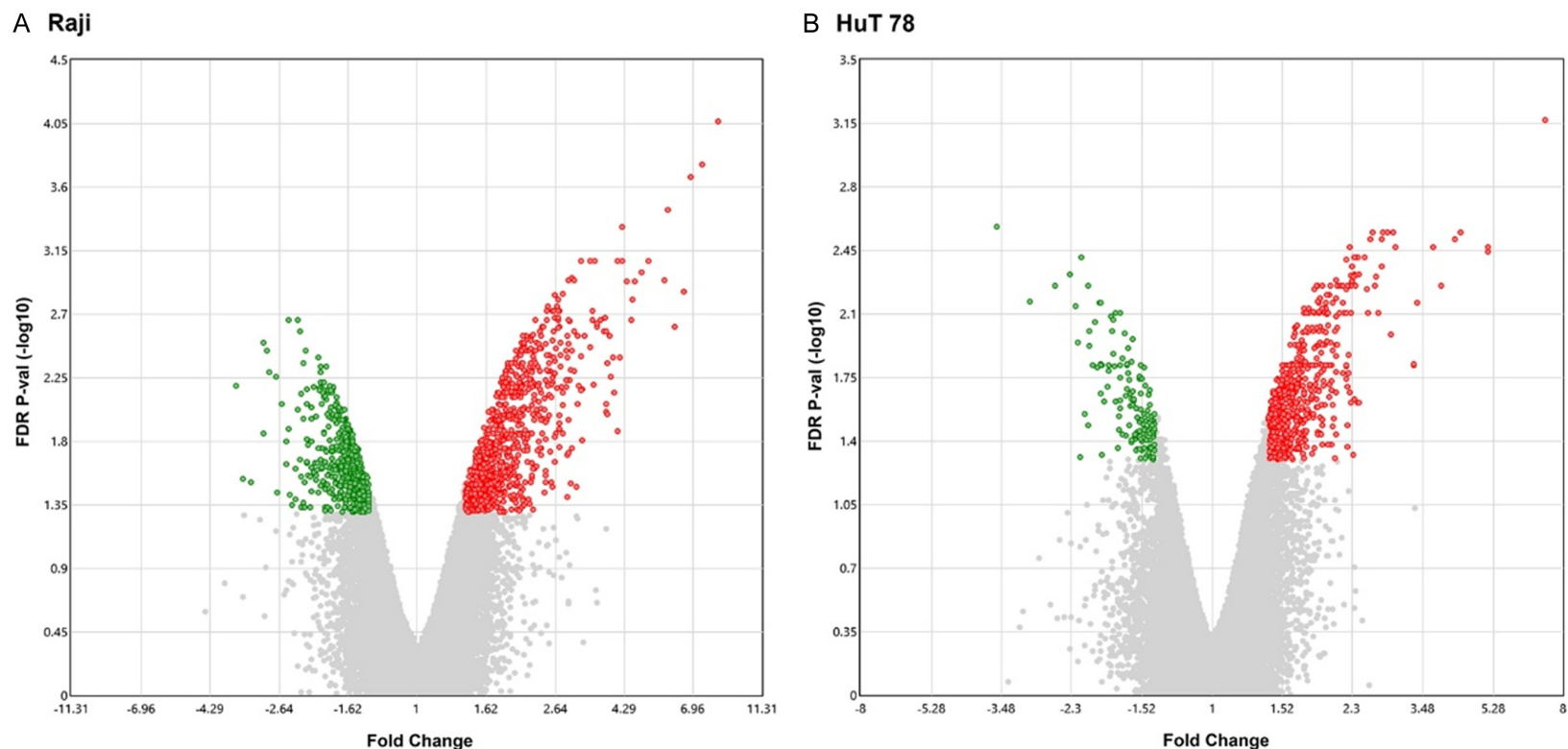
Figure 5. Volcano plot of differentially expressed genes with the hydralazine and valproate combination. Volcano plots show the differentially expressed genes in (A) Raji and (B) HuT 78 cell lines. Differentially expressed genes were selected by FDR<0.05 and a fold change >1.4 or <-1.4.

Table 1. List of the top ten up-regulated genes in HuT 78 and Raji cells, identified by volcano maps

Up-regulated	Down-regulated
PMAIP1, JUN, CD69, SLAMF7, TPMT, MIR21, CAMSAP2, WIPI1, SYT11, ABHD4, CLEC7A, ABCA5, ADAMTS6, MAML2, ZSWIM6, PPP4R4, TANC2, DPYD, ARID5B, LAMC1, SLC9A9, FMNL2, RGS9, LINC00936, PAIP2B, BBS9, CTTNBP2NL, ARRDC3, LOC105371220, PLEKHH2, LIMA1, SGCB, NPC2, ATP8B2, DOCK4, RALGAPA2, ILDR2, DYNC2H1, LOC154761, SRGN, RRAGD, FMO4, BCL2A1, CLEC2B, TSPAN33, FAM102B, GRAMD1C, EXOC6B, ST3GAL5, INPP4B, SRGAP2, CEP126, CPEB4, RGS1, NEO1, KLF6, FIG4, DZIP3, NABP1, ADGRL1, SLC30A4, REPS2, LINC01268, PAPSS1, YPEL5, MYO1D, SAMD9L, ATXN1, RPS6KC1, GLIPR1, IL18RAP, MBNL2, SLC12A6, IFI6, LYST, IFI44, OAS1, SLAMF6, NCF2, LMBRD2, TMEM154, HIVEP3, HIP1, SLC46A3, ATP1B1, DNAJC1, ERO1B, NRN1, ARHGAP18, PGM2L1, NFE2L3, ID: 16748202	RPS25, AVEN, GEMIN4, ACACA, USE1, SLC5A6, FAM136A, GTF3C6, LOC100506458, ID: 17122436

Table 2. Genes expressed in both cell lines, HuT 78 and Raji, 92 genes up-regulated and 10 genes down-regulated using Affymetrix Transcriptome Analysis Console software (version 4.0)

Cell line	Up-regulated genes	Expression fold-change value	Down-regulated genes	Expression fold-change value
Raji	CXCL10	8.180	NEIL1	-3.445
	IFI6	7.307	CEP152	-2.769
	DDX60	6.958	SNHG1	-2.690
	CD69	5.468	HSPA9	-2.441
	SAMD9L	5.311	mir-590	-2.325
	IFIT1	4.999	mir-573	-2.309
	IFI44	4.708	TRIP13	-2.272
	FAM49A	4.440	RPS25	-2.255
	DNAJC5B	4.303	CDC20	-2.213
	STAT1	4.282	LOC101928323	-2.178
HuT 78	SUCNR1	7.069	MUC1	-3.357
	CYP1A1	4.455	CXCR3	-2.953
	TLR6	4.168	NKG7	-2.450
	WASF1	4.156	NSMF	-2.264
	KIAA0408	3.939	COL6A1	-2.264
	SLCO4C1	3.868	SUSD4	-2.189
	LAIR2	3.520	PRSS57	-2.186
	NLRP1	3.297	TLR5	-2.118
	GBP2	3.102	GZMK	-2.088
	SLAMF7	3.015	LGMN	-2.064
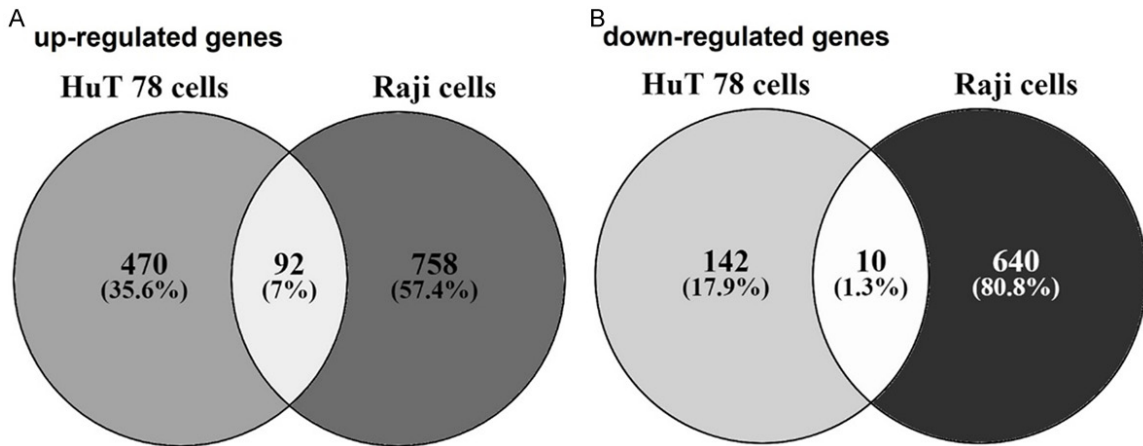
Figure 6. Venn diagram of the differentially regulated genes. The diagram illustrates the number of genes (A) upregulated and (B) downregulated in HuT 78 and Raji cell lines. The intersection in light color represents the expression of common genes between the two datasets.

cell cycle and apoptosis genes were also differentially expressed in both cell lines (Supplementary Tables 1, 2, 3 and 4). Table 2 and Figure 6 show the 92 genes up-regulated in both cell lines, whereas the 10 were down-regulated. The results show the complete list of up and down-regulated genes in both cell lines (Supplementary Tables 1, 2, 3 and 4). The qRT-PCR validation of FASN and SCD for HuT 78 and STAT1 for Raji cells confirmed the expression changes observed in the microarray (Figure 7).

Discussion

This study's findings, demonstrating the significant reduction in cell viability in lymphoma cell
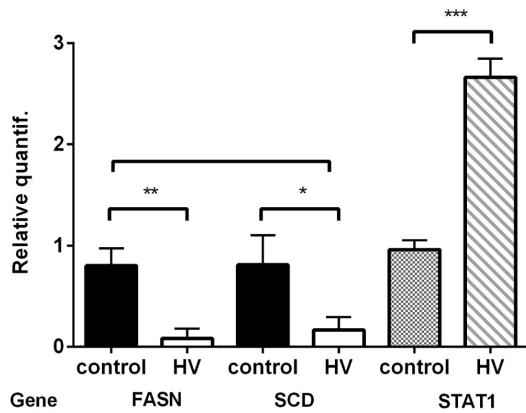
Figure 7. Validation of gene expression by qRT-PCR. The analysis of FASN and SCD for HuT 78 (bars black and white), and STAT1 for Raji cells (bars with patterns) confirmed the expression changes observed in the microarray. Statistically significant differences were determined for FASN (**, P = 0.0032) and SCD (*, P = 0.0256), as well as for STAT1 (***, P = 0.0001) as determined by an unpaired t test with a significance level of (P<0.05).

lines and the induction of cell cycle arrest and apoptosis through the combination of HV, hold promising potential for your work. Individually, these drugs exhibit cell viability inhibition, and their synergy can potentiate this effect. The microarray analysis revealed differential gene expression of 1.5% and 3.3% of the total genes, with the majority being up-regulated, 562 and 850, in HuT 78 and Raji cells, respectively. Three and five of the 10 most up-regulated genes in HuT 78 and Raji cells were related to immune function, further emphasizing the relevance of these findings for immunotherapy of lymphomas.

The current evidence underscores the prevalence of epigenetic derangements in both B-cell and T-cell lymphomas. These derangements not only contribute to lymphomagenesis but also play a role in treatment resistance. Given the common observation of alterations in DNA methylation and histone acetylation patterns in lymphomas, numerous preclinical and clinical studies have explored combinations of DNMTi with HDACi. Preclinical studies have shown that the combination of vorinostat with decitabine is not only cytotoxic in resistant lymphoma cells but also exhibits a synergistic effect [26]. This has been observed in various lymphoma models, including DLBCL and CTCL [28, 29].

In the clinical setting, there are at least 21 planned and ongoing phase I and II clinical studies that have evaluated the combination of a DNMTi (decitabine or azacitidine) or HDACi plus chemotherapy, showing variable efficacy, but with an increase in hematological toxicity [30]. Given the synergy between these two types of agents, a phase I study in patients with refractory solid tumors and lymphomas reported that the combination of decitabine with vorinostat is feasible and led to stable disease for four cycles in more than 11 (29%) out of 38 evaluable patients [31]. Double epigenetic modulation with vorinostat and azacitidine with the high-dose regimen gemcitabine/busulfan/melphalan was successfully tested in 60 patients, including 26 DLBCL (10 double hit/double expression), 21 with Hodgkin lymphoma, 8 with T-cell lymphoma, and 5 with other B-cell lymphomas. The toxicity profile was manageable, and neutrophils and platelets engrafted promptly. At a median follow-up of 15 months (range, 8-27 months), the event-free and overall survival rates were 65% and 77%, respectively [29]. These results are encouraging and warrant further testing of double epigenetic modulation.

Though we have reported preclinical and clinical activity of combined hydralazine valproate treatment in HuT 78 and CTCL patients [9, 27], there has been no evidence of its activity for B-cell lymphomas until now. Notably, cell viability was inhibited in the B-cells at seven days of treatment. In contrast, inhibition of T-cells was only 68%, suggesting that the combination could be even more active in B-cell lymphomas. However, this requires further studies. The apoptotic effects observed are in line with the treatment-induced up-regulation in Raji cells of *TNFSF10*, *FAS*, *TP63*, *PMAIP1*, *XAF1*, and *TP53INP1*, as well as the down-regulation of *BIRC5*, which is a member of the IAP family that interacts with BIRC4 and DIABLO to inactivate caspases 3 and 9 [32-36]. Additionally, the proapoptotic genes APAF1, *TP53I11*, and *PMAIP1* were up-regulated in HuT 78, while the expression of *BCL3* was decreased [37-39]. Furthermore, the cell cycle arrest observed for Raji's and HuT 78 cells could be related to the up-regulation of *CDKN1B* and *CDKN1A*, respectively. Interestingly, among the 92 genes that shared up-regulation in both cell lines, JUN is a transcription factor of the AP-1 family. Accordingly, activating the signaling pathway JNK-AP-1 induces proapoptotic genes such as *TNF-alfa*, *FAS-L*, and *Bak* [40, 41]. Conversely,

the *ACACA* gene was down-regulated in both cell lines. This gene codes for the Acetyl-Co-A carboxylase alfa enzyme, the limiting step in malonyl-CoA synthesis for de novo fatty acid synthesis.

Although there are no reports on the expression of ACACA in lymphoma, inhibitors of this enzyme are being evaluated as antitumor agents [42]. Particularly in lymphoma, lipids' role in lymphomagenesis proves significant [43]. Additionally, inhibiting FASN, another limiting enzyme for de novo fatty acid synthesis, induces apoptosis in lymphoma [44]. Beyond the changes in gene expression that could explain the inhibitory effects on viability, mainly the increased apoptosis observed, it is noteworthy that 3 and 5 of the ten most up-regulated genes in HuT 78 and Raji cell lines, respectively, participate in immune function (antigen processing, innate immunity, and interferon signaling). Recognizing that in vitro treatment with these drugs is not a good model for establishing potential immunological mechanisms, it is known that in vivo epigenetic modifications may be partly responsible for immune evasion in lymphomas [45]. A current treatment strategy is the combination of epigenetic agents with checkpoint inhibitors, as they have been shown to synergize in vivo [46].

Hydralazine valproate combined is well-tolerated and comes with no or minimal myelosuppression [6-9]. This is of crucial relevance because it can be combined with chemotherapy. Moreover, the combination of hydralazine valproate seems more effective in HuT 78 cells and less toxic to peripheral blood lymphocytes than vorinostat decitabine [27]. In a recent study, the regimen of valproate with R-CHOP was found to be more effective than historical controls in the first-line therapy of DLBCL [22].

In summary, this study underscores the potential of the hydralazine and valproate combination to significantly enhance the armamentarium of lymphoma therapy. The study demonstrates that this combination effectively treats T-lymphoma and B-cell lymphoma, with B-cell lymphoma being the most common type of non-Hodgkin's lymphoma. The concentrations of hydralazine and valproate used in the study, 10 µM and 1 mM, respectively, are achievable in clinical practice. In a pharmacokinetic study involving healthy volunteers who received a single dose of hydralazine and magnesium valproate, we found that the area under the curve concentration (AUC) for hydralazine was 8 µM/h and 8.6 µM/h (for slow and fast acetylators, respectively). In contrast, the AUC for valproate was 13.7 mM/h, which is much higher than the tested concentration in vitro [47]. These findings highlight the need to further investigate the HV combination in T and B-cell lymphoma, either alone or in combination with cytotoxic and targeted therapies. The fact that these drugs are widely used in clinics for non-cancer conditions, have no patent, are cost-effective, and save lives, further emphasizes their potential to enrich the lymphoma therapy arsenal.

Acknowledgements

Disclosure of conflict of interest

None.

Address correspondence to: Alfonso Dueñas-González, Subdirection of Basic Research, Instituto Nacional de Cancerología (INCan), Tlalpan, Mexico City 14080, Mexico. E-mail: alfonso_duenasg@yahoo.com

References

[1] Hassler MR, Schiefer AI and Egger G. Combating the epigenome: epigenetic drugs against non-Hodgkin's lymphoma. Epigenomics 2013; 5: 397-415.

[2] Lue JK, Amengual JE and O'Connor OA. Epigenetics and lymphoma: can we use epigenetics to prime or reset chemoresistant lymphoma programs? Curr Oncol Rep 2015; 17: 40.

[3] Sermer D, Pasqualucci L, Wendel HG, Melnick A and Younes A. Emerging epigenetic-modulating therapies in lymphoma. Nat Rev Clin Oncol 2019; 16: 494-507.

[4] Zambrano P, Segura-Pacheco B, Perez-Cardenas E, Cetina L, Revilla-Vazquez A, Taja-Chayeb L, Chavez-Blanco A, Angeles E, Cabrera G, Sandoval K, Trejo-Becerril C, Chanona-Vilchis J and Duenas-Gonzalez A. A phase I study of hydralazine to demethylate and reactivate the expression of tumor suppressor genes. BMC Cancer 2005; 5: 44.

[5] Chavez-Blanco A, Segura-Pacheco B, Perez-Cardenas E, Taja-Chayeb L, Cetina L, Candelaria M, Cantu D, Gonzalez-Fierro A, Garcia-Lo-

pez P, Zambrano P, Perez-Plasencia C, Cabrera G, Trejo-Becerril C, Angeles E and Duenas-Gonzalez A. Histone acetylation and histone deacetylase activity of magnesium valproate in tumor and peripheral blood of patients with cervical cancer. A phase I study. Mol Cancer 2005; 4: 22.

[6] Bauman J, Shaheen M, Verschraegen CF, Belinsky SA, Houman Fekrazad M, Lee FC, Rabinowitz I, Ravindranathan M and Jones DV Jr. A phase I protocol of hydralazine and valproic acid in advanced, previously treated solid cancers. Transl Oncol 2014; 7: 349-354.

[7] Candelaria M, Herrera A, Labardini J, Gonzalez-Fierro A, Trejo-Becerril C, Taja-Chayeb L, Perez-Cardenas E, de la Cruz-Hernandez E, Arias-Bofill D, Vidal S, Cervera E and Duenas-Gonzalez A. Hydralazine and magnesium valproate as epigenetic treatment for myelodysplastic syndrome. Preliminary results of a phase-II trial. Ann Hematol 2011; 90: 379-387.

[8] Candelaria M, Burgos S, Ponce M, Espinoza R and Duenas-Gonzalez A. Encouraging results with the compassionate use of hydralazine/valproate (TRANSKRIP) as epigenetic treatment for myelodysplastic syndrome (MDS). Ann Hematol 2017; 96: 1825-1832.

[9] Espinoza-Zamora JR, Labardini-Mendez J, Sosa-Espinoza A, Lopez-Gonzalez C, Vieyra-Garcia M, Candelaria M, Lozano-Zavaleta V, Toledano-Cuevas DV, Zapata-Canto N, Cervera E and Duenas-Gonzalez A. Efficacy of hydralazine and valproate in cutaneous T-cell lymphoma, a phase II study. Expert Opin Investig Drugs 2017; 26: 481-487.

[10] Malik A, Shoukier M, Garcia-Manero G, Wierda W, Cortes J, Bickel S, Keating MJ and Estrov Z. Azacitidine in fludarabine-refractory chronic lymphocytic leukemia: a phase II study. Clin Lymphoma Myeloma Leuk 2013; 13: 292-295.

[11] Blum KA, Liu Z, Lucas DM, Chen P, Xie Z, Baiocchi R, Benson DM, Devine SM, Jones J, Andritsos L, Flynn J, Plass C, Marcucci G, Chan KK, Grever MR and Byrd JC. Phase I trial of low dose decitabine targeting DNA hypermethylation in patients with chronic lymphocytic leukaemia and non-Hodgkin lymphoma: dose-limiting myelosuppression without evidence of DNA hypomethylation. Br J Haematol 2010; 150: 189-195.

[12] Fan H, Lu X, Wang X, Liu Y, Guo B, Zhang Y, Zhang W, Nie J, Feng K, Chen M, Zhang Y, Wang Y, Shi F, Fu X, Zhu H and Han W. Low-dose decitabine-based chemoimmunotherapy for patients with refractory advanced solid tumors: a phase I/II report. J Immunol Res 2014; 2014: 371087.

[13] Clozel T, Yang S, Elstrom RL, Tam W, Martin P, Kormaksson M, Banerjee S, Vasanthakumar A, Culjkovic B, Scott DW, Wyman S, Leser M, Shaknovich R, Chadburn A, Tabbo F, Godley LA, Gascoyne RD, Borden KL, Inghirami G, Leonard JP, Melnick A and Cerchietti L. Mechanism-based epigenetic chemosensitization therapy of diffuse large B-cell lymphoma. Cancer Discov 2013; 3: 1002-1019.

[14] Martin P, Bartlett NL, Chavez JC, Reagan JL, Smith SM, LaCasce AS, Jones J, Drew J, Wu C, Mulvey E, Revuelta MV, Cerchietti L and Leonard JP. Phase 1 study of oral azacitidine (CC-486) plus R-CHOP in previously untreated intermediate- to high-risk DLBCL. Blood 2022; 139: 1147-1159.

[15] Ogura M, Ando K, Suzuki T, Ishizawa K, Oh SY, Itoh K, Yamamoto K, Au WY, Tien HF, Matsuno Y, Terauchi T, Yamamoto K, Mori M, Tanaka Y, Shimamoto T, Tobinai K and Kim WS. A multicentre phase II study of vorinostat in patients with relapsed or refractory indolent B-cell non-Hodgkin lymphoma and mantle cell lymphoma. Br J Haematol 2014; 165: 768-776.

[16] Kirschbaum M, Frankel P, Popplewell L, Zain J, Delioukina M, Pullarkat V, Matsuoka D, Pulone B, Rotter AJ, Espinoza-Delgado I, Nademanee A, Forman SJ, Gandara D and Newman E. Phase II study of vorinostat for treatment of relapsed or refractory indolent non-Hodgkin's lymphoma and mantle cell lymphoma. J Clin Oncol 2011; 29: 1198-1203.

[17] Chen R, Frankel P, Popplewell L, Siddiqi T, Ruel N, Rotter A, Thomas SH, Mott M, Nathwani N, Htut M, Nademanee A, Forman SJ and Kirschbaum M. A phase II study of vorinostat and rituximab for treatment of newly diagnosed and relapsed/refractory indolent non-Hodgkin lymphoma. Haematologica 2015; 100: 357-362.

[18] Tan D, Phipps C, Hwang WY, Tan SY, Yeap CH, Chan YH, Tay K, Lim ST, Lee YS, Kumar SG, Ng SC, Fadilah S, Kim WS and Goh YT; SGH651 Investigators. Panobinostat in combination with bortezomib in patients with relapsed or refractory peripheral T-cell lymphoma: an open-label, multicentre phase 2 trial. Lancet Haematol 2015; 2: e326-333.

[19] Persky DO, Li H, Rimsza LM, Barr PM, Popplewell LL, Bane CL, Von Gehr A, LeBlanc M, Fisher RI, Smith SM and Friedberg JW. A phase I/II trial of vorinostat (SAHA) in combination with rituximab-CHOP in patients with newly diagnosed advanced stage diffuse large B-cell lymphoma (DLBCL): SWOG S0806. Am J Hematol 2018; 93: 486-493.

[20] Budde LE, Zhang MM, Shustov AR, Pagel JM, Gooley TA, Oliveira GR, Chen TL, Knudsen NL, Roden JE, Kammerer BE, Frayo SL, Warr TA,

Boyd TE, Press OW and Gopal AK. A phase I study of pulse high-dose vorinostat (V) plus rituximab (R), ifosphamide, carboplatin, and etoposide (ICE) in patients with relapsed lymphoma. Br J Haematol 2013; 161: 183-191.

[21] Hu B, Younes A, Westin JR, Turturro F, Claret L, Feng L, Fowler N, Neelapu S, Romaguera J, Hagemeister FB, Rodriguez MA, Samaniego F, Fayad LE, Copeland AR, Nastoupil LJ, Nieto Y, Fanale MA and Oki Y. Phase-I and randomized phase-II trial of panobinostat in combination with ICE (ifosfamide, carboplatin, etoposide) in relapsed or refractory classical Hodgkin lymphoma. Leuk Lymphoma 2018; 59: 863-870.

[22] Drott K, Hagberg H, Papworth K, Relander T and Jerkeman M. Valproate in combination with rituximab and CHOP as first-line therapy in diffuse large B-cell lymphoma (VALFRID). Blood Adv 2018; 2: 1386-1392.

[23] Gore SD. In vitro basis for treatment with hypomethylating agents and histone deacetylase inhibitors: can epigenetic changes be used to monitor treatment? Leuk Res 2009; 33 Suppl 2: S2-6.

[24] Hellebrekers DM, Griffioen AW and van Engeland M. Dual targeting of epigenetic therapy in cancer. Biochim Biophys Acta 2007; 1775: 76-91.

[25] Xu QY and Yu L. Epigenetic therapies in acute myeloid leukemia: the role of hypomethylating agents, histone deacetylase inhibitors and the combination of hypomethylating agents with histone deacetylase inhibitors. Chin Med J (Engl) 2020; 133: 699-715.

[26] Pera B, Tang T, Marullo R, Yang SN, Ahn H, Patel J, Elstrom R, Ruan J, Furman R, Leonard J, Cerchietti L and Martin P. Combinatorial epigenetic therapy in diffuse large B cell lymphoma pre-clinical models and patients. Clin Epigenetics 2016; 8: 79.

[27] Schcolnik-Cabrera A, Dominguez-Gomez G and Duenas-Gonzalez A. Comparison of DNA demethylating and histone deacetylase inhibitors hydralazine-valproate versus vorinostat-decitabine incutaneous T-cell lymphoma in HUT78 cells. Am J Blood Res 2018; 8: 5-16.

[28] Kalac M, Scotto L, Marchi E, Amengual J, Seshan VE, Bhagat G, Ulahannan N, Leshchenko VV, Temkin AM, Parekh S, Tycko B and O'Connor OA. HDAC inhibitors and decitabine are highly synergistic and associated with unique gene-expression and epigenetic profiles in models of DLBCL. Blood 2011; 118: 5506-5516.

[29] Nieto Y, Valdez BC, Thall PF, Jones RB, Wei W, Myers A, Hosing C, Ahmed S, Popat U, Shpall EJ, Qazilbash M, Gulbis A, Anderlini P, Shah N, Bashir Q, Alousi A, Oki Y, Fanale M, Dabaja B, Pinnix C, Champlin R and Andersson BS. Double epigenetic modulation of high-dose chemotherapy with azacitidine and vorinostat for patients with refractory or poor-risk relapsed lymphoma. Cancer 2016; 122: 2680-2688.

[30] Amengual JE. Can we use epigenetics to prime chemoresistant lymphomas? Hematology Am Soc Hematol Educ Program 2020; 2020: 85-94.

[31] Stathis A, Hotte SJ, Chen EX, Hirte HW, Oza AM, Moretto P, Webster S, Laughlin A, Stayner LA, McGill S, Wang L, Zhang WJ, Espinoza-Delgado I, Holleran JL, Egorin MJ and Siu LL. Phase I study of decitabine in combination with vorinostat in patients with advanced solid tumors and non-Hodgkin's lymphomas. Clin Cancer Res 2009; 27: 3528.

[32] Valentin R, Grabow S and Davids MS. The rise of apoptosis: targeting apoptosis in hematologic malignancies. Blood 2018; 132: 1248-1264.

[33] Klanova M and Klener P. BCL-2 proteins in pathogenesis and therapy of B-cell non-hodgkin lymphomas. Cancers (Basel) 2020; 12: 938.

[34] Deng J. How to unleash mitochondrial apoptotic blockades to kill cancers? Acta Pharm Sin B 2017; 7: 18-26.

[35] Zhang L and Fang B. Mechanisms of resistance to TRAIL-induced apoptosis in cancer. Cancer Gene Ther 2005; 12: 228-237.

[36] van Keimpema M, Gruneberg LJ, Mokry M, van Boxtel R, Koster J, Coffer PJ, Pals ST and Spaargaren M. FOXP1 directly represses transcription of proapoptotic genes and cooperates with NF-kappaB to promote survival of human B cells. Blood 2014; 124: 3431-3440.

[37] Cain K. Chemical-induced apoptosis: formation of the Apaf-1 apoptosome. Drug Metab Rev 2003; 35: 337-363.

[38] Liang XQ, Cao EH, Zhang Y and Qin JF. A P53 target gene, PIG11, contributes to chemosensitivity of cells to arsenic trioxide. FEBS Lett 2004; 569: 94-98.

[39] Jin S, Cojocari D, Purkal JJ, Popovic R, Talaty NN, Xiao Y, Solomon LR, Boghaert ER, Leverson JD and Phillips DC. 5-azacitidine induces NOXA to prime AML cells for venetoclax-mediated apoptosis. Clin Cancer Res 2020; 26: 3371-3383.

[40] Dhanasekaran DN and Reddy EP. JNK signaling in apoptosis. Oncogene 2008; 27: 6245-6251.

[41] Feng Z and Wang J. Soluble CD40 ligand inhibits the growth of non-Hodgkin's lymphoma cells through the JNK signaling pathway. Oncol Lett 2021; 21: 56.

[42] Huang T, Wu X, Yan S, Liu T and Yin X. Synthesis and in vitro evaluation of novel spiroketopyrazoles as acetyl-CoA carboxylase inhibitors and potential antitumor agents. Eur J Med Chem 2021; 212: 113036.

[43] Guo W, Wang X, Li Y and Bai O. Function and regulation of lipid signaling in lymphomagenesis: a novel target in cancer research and therapy. Crit Rev Oncol Hematol 2020; 154: 103071.

[44] Kant S, Kumar A and Singh SM. Tumor growth retardation and chemosensitizing action of fatty acid synthase inhibitor orlistat on T cell lymphoma: implication of reconstituted tumor microenvironment and multidrug resistance phenotype. Biochim Biophys Acta 2014; 1840: 294-302.

[45] Di Pietro A and Good-Jacobson KL. Disrupting the code: epigenetic dysregulation of lymphocyte function during infectious disease and lymphoma development. J Immunol 2018; 201: 1109-1118.

[46] Chen X, Pan X, Zhang W, Guo H, Cheng S, He Q, Yang B and Ding L. Epigenetic strategies synergize with PD-L1/PD-1 targeted cancer immunotherapies to enhance antitumor responses. Acta Pharm Sin B 2020; 10: 723-733.

[47] Garces-Eisele SJ, Cedillo-Carvallo B, Reyes-Nunez V, Estrada-Marin L, Vazquez-Perez R, Juarez-Calderon M, Guzman-Garcia MO, Duenas-Gonzalez A and Ruiz-Arguelles A. Genetic selection of volunteers and concomitant dose adjustment leads to comparable hydralazine/valproate exposure. J Clin Pharm Ther 2014; 39: 368-375.